A quartz crystal microbalance with dissipation monitoring of dehydrogenative copolymerization of coniferyl alcohol and sinapyl alcohol

Shoichi Sato[a], Shiori Suzuki[b], Kengo Shigetomi[b]*, and Yasumitsu Uraki[b]

[a]*Graduate School of Agriculture, Hokkaido University, Kita 9, Nishi 9, Kita-ku, Sapporo 060-8589, Japan;* [b]*Research faculty of Agriculture, Hokkaido University, Kita 9, Nishi 9, Kita-ku, Sapporo 060-8589, Japan*

*E-mail: sgtm@agr.hokudai.ac.jp, Tel: +81-11-706-2818

A quartz crystal microbalance with dissipation monitoring of dehydrogenative copolymerization of coniferyl alcohol and sinapyl alcohol

Dehydrogenation polymers (DHPs) can be prepared from coniferyl alcohol (CA), but not solely from sinapyl alcohol (SA) when catalyzed by horseradish peroxidase (HRP). However, it has been proven that from a mixture of CA and SA, DHP with SA incorporated can be formed even with HRP. Conventional experiments using this mixed monolignol system required large amounts of monolignols and enzymes. The use of a quartz crystal microbalance with dissipation (QCM-D) can overcome this drawback. In this study, the dehydrogenative copolymerization of small amounts of CA/SA mixtures and HRP was performed on a QCM-D to further explore the benefits of this system. The DHPs were successfully formed from mixed monolignols on the QCM-D system, and the incorporation of the SA unit was verified through differences in DHP formation between binary monolignol systems and the corresponding CA-single systems. The formation of DHP in the presence of the polysaccharide matrix was performed at the same reaction scale, and the promotional effect of partially acetylated xylan on DHP formation was observed, especially at high CA ratios. The QCM-D monitoring system will be a valuable tool for analyses under limited substrates and/or enzymes that may be encountered in the future.

Keywords: QCM-D; dehydrogenation polymer; sinapyl alcohol

Introduction

A quartz crystal microbalance (QCM) is a technology that enables the real-time quantification of adsorbates on its sensor surface by utilizing the inverse piezoelectric effect of quartz crystals in an electric field. One notable advantage of this method is its ability to detect slight mass difference, *e.g.*, 17.7 ng/cm^2/Hz for a 5 MHz crystal.[1] In addition, when the QCM is coupled with dissipation monitoring, known as QCM-D, it not only provides information about the mass adsorbed on a sensor surface but also offers insights into the viscoelastic behavior of the layer generated by adsorbed materials on a

sensor surface through the measurement of the dissipation factor. QCM-D is widely used to investigate the interactions between macromolecules and substrates, such as cellulose derivatives and inorganics, cell membranes and lignin small molecules, and so on.[2–5] In addition, Wang et al.[6] monitored the dehydrogenative polymerization of small doses of monolignols (14 μmol) initiated by horseradish peroxidase (HRP) immobilized on sensor surfaces in real time using QCM-D, demonstrating that dehydrogenation polymers (DHPs) could be successfully obtained from coniferyl alcohol (CA) but not from sinapyl alcohol (SA) using HRP.

In trees, cell walls are constructed by depositing hemicellulose onto cellulose to form a polysaccharide matrix, which is then followed by the lignification in the matrix.[7] QCM-D has also been employed to investigate hemicellulose adsorption on cellulose model sensor surfaces that mimic cell wall formation.[8–13] Lyu et al.[14, 15] combined the fabrication of artificial polysaccharide matrices on a sensor surface with the tracking of dehydrogenative polymerization using QCM-D to investigate the effect of polysaccharides on lignification. They demonstrated that the presence of partially acetylated xylan (AcXY) with acetyl groups having an acetyl content similar to that of native hardwood xylan significantly enhances the formation of DHP from CA by HRP, in comparison to non-acetylated xylan and other polysaccharides. QCM-D has enabled the tracking of dehydrogenative polymerization from small amounts of samples (8.1 μmol of monolignols and 150 μg of HRP for one experiment) and in polysaccharide matrices.

Kishimoto et al.[16] produced DHPs in a buffered solution using endwise polymerization (Zutropfverfahren, a gradual monolignol addition method) from mixtures of CA and SA under HRP catalysis, demonstrating that DHPs with incorporated syringyl units were formed even with the HRP catalyst. This observation implies the possibility of a radical-mediating action from CA to SA. It should be noted that this experimental

system required a large quantity of substrates (1.5 mmol of substrates for one experiment) and an enzyme (2 mg) because of the subsequent need for structure elucidation, *i.e.*, alkaline nitrobenzene oxidation and thioacidolysis, to obtain the syringyl to guaiacyl (S/G) ratio of the resulting DHPs. This enzyme loading, *i.e.*, 2 mg per experiment, would not be a problem for HRP, as it is commercially available in sufficient quantities. However, HRP has a significant drawback of not being woody origin. As a wood-derived enzyme, a cationic cell wall-bound peroxidase (CWPO-C) was discovered in poplar (*Populus alba* L.) and found to be SA-specific.[17–20] Currently, recombinant CWPO-C, constructed through heterologous expression in *Escherichia coli* and subsequent refolding processes, is used in research.[15, 21, 22] If an enzyme specific for CA is discovered in hardwoods in the future, conventional dehydrogenative polymerization studies may face limitations that require a significant quantity of the enzyme for continuous experiments. Here, the use of QCM-D to overcome these limitations is reported on.

In this study, DHP formation from monolignol mixtures (CA and SA) was revisited using QCM-D monitoring to further explore the benefits of QCM-D. Cellulose nanofibers (CNFs) were anchored onto the QCM-D sensor surface first and HRP was subsequently adsorbed onto the CNF-coated sensor. Subsequently, the dehydrogenative copolymerization of CA and SA was attempted. Since QCM-D monitoring cannot determine the actual monomer composition of the resulting DHPs, DHP formation under CA-single conditions was conducted to verify the incorporation of SA based on the differences in adsorption. Similar experiments were performed on the CNF/AcXY matrix to investigate the effect of AcXY on the copolymerization of CA and SA.

Experimental

Materials

CA and SA were synthesized according to a previously reported method.[23] AcXY, with a degree of acetylation of 0.50 was prepared from commercial beech xylan.[15] CNFs as a 2% hydrogel, which was prepared by the mechanical defibration of hardwood kraft pulp, was supplied by Hokuetsu Corporation (Tokyo, Japan) and used after purification.[14] HRP (503 units/mg for tetraguaiacol generated from guaiacol) was purchased from FUJIFILM Wako Pure Chemical Industries (Osaka, Japan) and used as received.

QCM-D measurements

CNF-coated QCM-D sensors were prepared as described previously.[14] Briefly, 5 MHz AT-cut quartz crystal sensors (QSX 303, Q-sense AB) with a silicon oxide surface were used. 3-aminopropyltrimethoxysilane (APTS) was first coated onto the sensor surface by spin-coater Labo-coat (ncx, Tokyo, Japan), followed by the spin-coating of CNFs suspension. The frequency change (Δf) of the sensor before and after CNF deposition was measured using QSense Explorer (Biolin Scientific, Västra Frölunda, Sweden). The dried amount of CNFs deposited on the sensor was calculated using the Sauerbrey equation (equation (1))[24]:

$$\Delta m = -C \frac{\Delta f}{n} \quad (1)$$

where Δm (ng/cm^2) is the weight change, C is the mass sensitivity constant of the sensor (17.7 ng/cm^2/Hz), and n is the overtone number (n = 5 in this study). The CNF coating procedure was repeated until Δm exceeded 4000 ng/cm^2 after drying, when the CNFs theoretically covered the entire surface of the sensor as a monolayer.[14, 25]

All the QCM-D measurements were performed at 25 °C under a constant flow rate (50 μL/min) controlled by a peristaltic pump ISM795C (ISMATEC, Glattbrugg-Zürich, Switzerland). The changes in Δf and dissipation factor (ΔD) of the sensor were monitored during the measurements. The dissipation factor (D) is defined by the following equation[26]:

$$D = \frac{E_{diss}}{2\pi E_{stored}} \quad (2)$$

where E_{diss} is the dissipated energy and E_{stored} is the stored energy during one oscillation.

The dried CNF-coated sensor was placed in a measurement cell and conditioned with Milli-Q water. Next, an aqueous solution of AcXY (1.0 g/L) was introduced into the cell for 2 h. Milli-Q water was subsequently introduced for 15 min to remove unbound AcXY.

CNF-coated sensors, with or without AcXY adsorption, were equilibrated with phosphate-buffered saline (PBS, pH 6.1, 10 mM phosphate containing 0.8% *w*/*v* NaCl and 0.02% *w*/*v* KCl). HRP in PBS at a concentration of 0.10 g/L was then introduced for 30 min, followed by rinsing with PBS for 15 min. Each monolignol solution (total 2.70 mM; CA:SA = 0.81 mM:1.89 mM, 1.35:1.35, and 1.89:0.81; their corresponding CA:SA molar ratios are 3:7, 5:5, and 7:3, respectively) in PBS containing 2.70 mM of H_2O_2 was introduced into the cell for 1 h. The sensor surface was then rinsed successively with PBS for 15 min. As a CA-single system corresponding to the mixed system, 0.81, 1.35, and 1.89 mM of CA solutions with 2.70 mM of H_2O_2 in PBS were also tested in the same manner. For references, 2.70 mM of CA solution with or without H_2O_2 was introduced into the CNF-coated sensor after HRP adsorption.

Atomic force microscope (AFM) imaging

The sensors after the QCM-D measurement were dried under a N_2 flow and observed using SPA-400 AFM (HITACHI High-Tech Science, Kyoto, Japan) and expressed as shape images.

Results and discussion

Adsorption of HRP on polysaccharides

Prior to the formation of DHP, HRP was immobilized on CNF- or CNF/AcXY-coated sensors.[15] Following the procedures in our previous report, CNFs were first coated on the QCM-D sensor (SiO_2) with APTS as an anchoring layer. [14] The deposited amount of the CNFs was calculated based on the Δf value of the dried CNFs-coated sensor to be more than 4000 ng/cm^2. This value was high enough for the theoretical amount to indicate complete coverage of the sensor surface. AcXY, with a degree of acetylation of 0.50, was flowed into a CNF-coated sensor in QCM-D to fabricate a CNF/AcXY-coated sensor.[15] The adsorption of HRP on the polysaccharides was monitored by flowing an HRP solution into the measurement cell. The QCM-D profiles are presented in Figure 1. In Figure 1A, Δf/n is plotted versus flow time, where a smaller Δf/n indicates a larger amount of adsorption onto the sensors. It should be noted that determining the accurate mass of the adsorbates is difficult only from the Δf/n plot because the adsorption of solvents can partly affect the change in Δf/n value. The ΔD-Δf/n plots are shown in Figure 1B. This plot reflects the viscoelastic changes with respect to the amount of adsorption (Δf/n) on the sensor surface.[10, 27] Specifically, a decrease in ΔD with a change in Δf/n value indicates the formation of a rigid layer, often a hydrophobic environment on the sensor surface, whereas an increase suggests the formation of a softer layer, often caused by hydration. The amount of HRP adsorbed onto the CNF/AcXY-coated sensor was lower

than that adsorbed onto the CNFs alone (Figure 1A), which is consistent with the findings of a previous study.[15] The ΔD-Δf/n plots indicated that HRP adsorption provided unchanged or rather rigid surface on the sensors (Figure 1B). Therefore, the effect of water adsorption is not significant on the mass change and the slightly higher adsorption on the CNF-coated sensor can be interpreted as due solely to the adsorption of HRP. The lower adsorption on the CNF/AcXY-coated sensor may be explained by the prevention of potential hydrogen bonding interactions between CNFs and HRP due to partially acetylated xylan.

Dehydrogenative copolymerization of CA and SA on CNF matrix

The formation of DHPs from a mixed system of monolignols, *i.e.*, CA and SA, was investigated using CNF-coated and HRP-adsorbed sensors. Mixed solutions of CA and SA at molar ratios of 3:7, 5:5, and 7:3 (total concentration of 2.70 mM) were flowed into the measurement cells along with 2.70 mM H_2O_2 for a duration of 60 min. These QCM-D profiles are shown in Figure 2A and the maximum absolute Δf/n values ($|\Delta f/n|$) are shown in Figure 2C. As references, the adsorptions of CA without H_2O_2 and SA without H_2O_2 were tested. Since the SA without H_2O_2 condition showed a similar Δf/n profile to that of CA without H_2O_2,[15] only the maximum absolute Δf/n value is displayed in Figure 2C. The Δf/n value obtained in CA with H_2O_2 condition are also displayed in Figure 2C as another reference. As shown in Figure 2A, CA without H_2O_2 condition exhibited a sharp drop by 24 Hz in 5 min, indicating the rapid adsorption of a monolignol. By contrast, the mixed systems with H_2O_2 exhibited a gradual decrease in Δf/n, which reached a plateau at -54 – -81 Hz in approximately 20 min. These distinct behaviors indicate the formation of DHPs on the sensor in the mixed system. In addition, increased DHP formation was observed at higher CA ratios in the mixed monolignol solutions, and

especially at higher SA ratios, DHP accumulation was less than that under CA with H_2O_2 condition (Figure 2C). This tendency is consistent with previous results obtained on a millimolar scale.[16] The DHP formation in the present mixed system was affirmed by AFM imaging of the resultant sensor surfaces: the particle matter that observed also in a previous study was seen only under the H_2O_2-supplemented condition (Figure 3).[6, 15]

The ΔD-Δf/n plots of the mixed systems are shown in Figure 2B. All the results showed two-phase profiles: steep curves up to approximately Δf/n = -20 Hz and shallow curves thereafter. The steep region indicates a significant softening of the surface, likely caused by the adsorption of hydrated monolignols, because the adsorption of water molecule can contribute to the softening. In the shallow curve region, the softening of the surface slowed owing to the development of hydrophobic DHP layers. Interestingly, the higher the CA ratio, the shallower was the slope, suggesting the formation of a more elastic surface for the same adsorption amount (Δf/n). These qualitative differences would be explained by differences in the monomer compositions of the resulting DHPs or by differences in their structures.

To detect the incorporation of SA into the resultant DHPs, DHP formations were attempted under CA-single conditions without SA, where only the same concentrations of CA as those in the mixed system were used, because QCM-D monitoring cannot directly determine the CA/SA ratio of the DHPs. ~~The maximum absolute Δf/n values (|Δf/n|) are shown in Figure 2C along with those of the first experiment (Figure 2A) and some reference experiments.~~ Under all conditions of the CA-single system, a decrease of more than 20 Hz in |Δf/n| was observed compared to the corresponding conditions containing SA (Figure 2C). Since the effect of SA on CA to promote DHP formation, i.*e*., radical transfer from SA to CA, is unlikely to occur from their difference in redox

potential,[19, 28] it can be concluded that the difference in |Δ*f*/n| is solely due to the incorporation of SA into the DHPs in the mixed system.

Effects of AcXY on copolymerization of CA and SA

The presence of AcXY has been shown to promote the formation of DHP prepared from CA alone through HRP catalysis.[15] Therefore, the effects of AcXY on the mixed monolignol system were examined.

The QCM-D results obtained using the same CA:SA ratios as in the previous experiments are shown in Figure 4A. A lower Δ*f*/n was observed when the higher the CA ratio in the mixed monolignols solutions on CNFs/AcXY, which was similar to that on CNFs alone. To compare the DHP adsorption amount between on CNFs and on CNFs/AcXY, the maximum |Δ*f*/n| values are shown in Figure 4C, along with those obtained on the CNF-coated sensor (Figure 2C). A lower |Δ*f*/n| was observed at a CA:SA ratio of 3:7 on CNFs/AcXY compared to that on the CNFs alone (45 Hz vs 54 Hz). This could be attributed to the slightly lower adsorption of HRP on AcXY than on the CNFs (Figure 1). In contrast, the maximum values of |Δ*f*/n| for the CNF/AcXY-coated sensors were higher at CA:SA ratios of 5:5 and 7:3 (80 and 85 Hz, respectively) compared to those of the CNFs alone. Despite the reduced enzyme adsorption on CNFs/AcXY compared to that on CNFs, the increase in DHP adsorption at these ratios could be attributed to the aforementioned promotional effect of AcXY. It was reported that the interactions of hemicelluloses with monolignols were primarily hydrophobic interactions.[29] Considering that CA is slightly more hydrophobic than SA,[30] CA would exhibit a higher affinity for AcXY, which is also hydrophobic,[31] and may facilitate the formation of DHP by the HRP catalyst.

The ΔD-Δf/n plots of the mixed system on AcXY are shown in Figure 4B. In the case of higher ratios of CA (CA:SA=5:5 and 7:3), similar profiles were observed, independent of the amount of SA, which would reflect the result that the promotion effect of AcXY became pronounced at higher CA ratios. On the other hand, at a lower CA ratio (CA:SA=3:7), the surface was more rigid than that at the same Δf/n (e.g., ΔD (10^{-6}) = 11.2 vs 13.6 at Δf/n = –40 Hz). In the comparison to the CA:SA=3:7 condition on the CNFs sensor (Figure 2B), the CNFs/AcXY condition resulted in a more rigid surface at the same Δf/n value (e.g., ΔD (10^{-6}) = 11.2 vs 12.9 at Δf/n = –40 Hz). Therefore, AcXY could affect both the quantity (Δf/n) and quality (ΔD) of the resultant DHPs in the CA/SA mixed system.

Conclusions

Conventional studies on dehydrogenative copolymerization from mixed monolignols have required large amounts of monolignols and enzymes, because the resulting DHPs was to be subjected to thioacidolysis and alkaline nitrobenzene oxidation to obtain the S/G ratio. To lower the amounts of samples required for analyses, the QCM-D system was applied to monitor a similar phenomenon, *i.e.*, the HRP-catalyzed dehydrogenative copolymerization of CA and SA. The results demonstrated that DHPs were successfully formed from the mixed monolignols in the QCM-D system, and the incorporation of SA into the DHP was confirmed by differences in DHP formation between the binary monolignol system and the corresponding CA-single system. On the AcXY/CNF sensor, which was prepared to mimic a lignification environment, DHP formation from the mixed monolignols was promoted compared to that on the CNF sensor, especially at high CA ratios. Hence, QCM-D monitoring enabled us to revisit the dehydrogenative copolymerization from a mixed-monolignol system, where the amount of substrate was

reduced to 1/185 and the amount of enzyme was reduced to 1/13 compared to the conventional method. Furthermore, this method can be used to easily fabricate a polysaccharide matrix, even with water-soluble polysaccharides such as pectin and cyclodextrin.[32, 33] This experimental system will serve as a valuable analytical tool, particularly when CA-specific peroxidases and/or oxidases are discovered and isolated from hardwood.

Acknowledgements

A part of this work was conducted at Laboratory of XPS analysis, Joint-use facilities, Hokkaido university. This work was supported by JSPS KAKENHI (Grant-in-Aid for Scientific Research (A)) under Grant Number JP21H04730.

Declaration of interest statement

The authors declare that they have no known competing financial interests or personal relationships that could have appeared to influence the work reported in this paper.

Data availability statement

All data generated or analyzed during this study are included in this published article.

References

[1] Easley, A. D.; Ma, T.; Eneh, C. I.; Yun, J.; Thakur, R. M.; Lutkenhaus, J. L.; A practical guide to quartz crystal microbalance with dissipation monitoring of thin polymer films. *J. Polym. Sci*. **2022**, *60* (7), 1090

[2] Nypelö, T.; Pynnönen, H.; Österberg, M.; Paltakari, J.; Laine, J. Interactions between Inorganic Nanoparticles and Cellulose Nanofibrils. *Cellulose*. **2012**, *19*, 779–792.

[3] Moradipour, M.; Tong, X.; Novak, B.; Kamali, P.; Asare, S. O.; Lynn, B. C.; Moldovan, D.; Rankin, S. E.; Knutson, B. L. Interaction of Lignin Dimers with

Model Cell Membranes: A Quartz Crystal Microbalance and Molecular Dynamics Simulation Study. *Biointerphases*. **2021**, *16*, 041003.

[4] Fatisson, J.; Ghoshal, S.; Tufenkji, N. Deposition of Carboxymethylcellulose-Coated Zero-Valent Iron Nanoparticles onto Silica: Roles of Solution Chemistry and Organic Molecules. *Langmuir*. **2010**, *26*, 12832–12840.

[5] Elschner, T.; Adam, J.; Lesny, H.; Joseph, Y.; Fischer, S. Growing of Artificial Lignin on Cellulose Ferulate Thin Films. *Biomacromolecules*. **2022**, *23*, 2089–2097.

[6] Wang, C.; Qian, C.; Roman, M.; Glasser, W. G.; Esker, A. R. Surface-Initiated Dehydrogenative Polymerization of Monolignols: A Quartz Crystal Microbalance with Dissipation Monitoring and Atomic Force Microscopy Study. *Biomacromolecules*. **2013**, *14*, 3964–3972.

[7] Terashima, N.; Fukushima, K.; He. L.-F.; Takabe, K. Comprehensive Model of the Lignified Plant Cell Wall. In Forage Cell Wall Structure and Digestibility; Jung, H. G.; Buxton, D. R.; Hatfield, R. D.; Ralph, J., Eds. American Society of Agronomy: Madison WI, 1993; pp 247-283.

[8] Benselfelt, T.; Cranston, E. D.; Ondaral, S.; Johansson, E.; Brumer, H.; Rutland, M. W.; Wågberg, L. Adsorption of Xyloglucan onto Cellulose Surfaces of Different Morphologies: An Entropy-Driven Process. *Biomacromolecules*. **2016**, *17*, 2801–2811.

[9] Eronen, P.; Österberg, M.; Heikkinen, S.; Tenkanen, M.; Laine, J. Interactions of Structurally Different Hemicelluloses with Nanofibrillar Cellulose. *Carbohydr. Polym.* **2011**, *86*, 1281–1290.

[10] Jaafar, Z.; Mazeau, K.; Boissière, A.; Le Gall, S.; Villares, A.; Vigouroux, J.; Beury, N.; Moreau, C.; Lahaye, M.; Cathala, B. Meaning of Xylan Acetylation on Xylan-Cellulose Interactions: A Quartz Crystal Microbalance with Dissipation (QCM-D) and Molecular Dynamic Study. *Carbohydr. Polym.* **2019**, *226*, 115315.

[11] Köhnke, T.; Östlund, A.; Brelid, H. Adsorption of Arabinoxylan on Cellulosic Surfaces: Influence of Degree of Substitution and Substitution Pattern on Adsorption Characteristics. *Biomacromolecules*. **2011**, *12*, 2633–2641.

[12] Kittle, J. D.; Qian, C.; Edgar, E.; Roman, M.; Esker, A. R. Adsorption of Xyloglucan onto Thin Films of Cellulose Nanocrystals and Amorphous Cellulose: Film Thickness Effects. *ACS Omega*. **2018**, *3*, 14004–14012.

[13] Yao, M.; Liang, C.; Yao, S.; Liu, Y.; Zhao, H.; Qin, C. Kinetics and Thermodynamics of Hemicellulose Adsorption onto Nanofibril Cellulose Surfaces by QCM-D. *ACS Omega*. **2021**, *6*, 30618–30626.

[14] Lyu, Y.; Matsumoto, T.; Taira, S.; Ijiri, K.; Yoshinaga, A.; Shigetomi, K.; Uraki, Y. Influences of Polysaccharides in Wood Cell Walls on Lignification In Vitro. *Cellulose*. **2021**, *28*, 9907–9917.

[15] Lyu, Y.; Suzuki, S.; Nagano, H.; Shigetomi, K.; Tamai, Y.; Tsutsumi, Y.; Uraki, Y. Effects of Hemicelluloses on Dehydrogenative Polymerization of Monolignols with Cationic Cell Wall-Bound Peroxidase. *Carbohydr. Polym.* **2023**, *301*, 120305.

[16] Kishimoto, T.; Chiba, W.; Saito, K.; Fukushima, K.; Uraki, Y.; Ubukata, M. Influence of Syringyl to Guaiacyl Ratio on the Structure of Natural and Synthetic Lignins. *J. Agric. Food Chem.* **2010**, *58*, 895–901.

[17] Tsutsumi, Y.; Nishida, T.; Sakai, K. Lignin Biosynthesis in Woody Angiosperm Tissue III. Isolation of Substrate-Specific Peroxidases Related the Dehydrogenative Polymerization of Sinapyl and Coniferyl Alcohols from Populous Callus Cultures. *Mokuzai Gakkaishi*. **1994**, *40*(12), 1348–1354.

[18] Sasaki, S.; Nishida, T.; Tsutsumi, Y.; Kondo, R. Lignin Dehydrogenative Polymerization Mechanism: A Poplar Cell Wall Peroxidase Directly Oxidizes Polymer Lignin and Produces In Vitro Dehydrogenative Polymer Rich in β-O-4 Linkage. *FEBS Lett.* **2004**, *562*, 197–201.

[19] Aoyama, W.; Sasaki, S.; Matsumura, S.; Mitsunaga, T.; Hirai, H.; Tsutsumi, Y.; Nishida, T. Sinapyl Alcohol-Specific Peroxidase Isoenzyme Catalyzes the Formation of the Dehydrogenative Polymer from Sinapyl Alcohol. *J. Wood Sci.* **2002**, 48, 497–504.

[20] Sasaki, S.; Nonaka, D.; Wariishi, H.; Tsutsumi, Y.; Kondo, R. Role of Tyr Residues on the Protein Surface of Cationic Cell-Wall-Peroxidase (CWPO-C) from Poplar: Potential Oxidation Sites for Oxidative Polymerization of Lignin. *Phytochemistry*. **2008**, *69*, 348–355.

[21] Shigeto, J.; Itoh, Y.; Tsutsumi, Y.; Kondo, R. Identification of Tyr74 and Tyr177 as Substrate Oxidation Sites in Cationic Cell Wall-Bound Peroxidase from Populus alba L. *FEBS Journal*. **2012**, *279*, 348–357.

[22] Yoshikay-Benitez, D. A.; Ohira, K.; Banerjee, K.; Fujita, K.; Shigeto, J.; Tsutsumi, Y. The Populus alba Cationic Cell-Wall-Bound Peroxidase (CWPO-C) Regulates Plant Growth, Lignin Content and Composition in Poplar. *J. Wood Sci.* **2023**, *69*.

[23] Quideau, S.; Ralph, J. Facile Large-Scale Synthesis of Coniferyl, Sinapyl, and p-Coumaryl Alcohol. *J. Agrlc. Food Chem.* **1992,** 40(7), 1108-1110.

[24] Sauerbrey, G; Verwendung von Schwingquarzen zur Wagung dunner Schichten und zur Mikrowagung. *Zeitschrift fur Physik.* **1959,** 155(2), 206-222.

[25] Sugiyama, J.; Vuong, R.; Chanzy, H. Electron Diffraction Study on the Two Crystalline Phases Occurring in Native Cellulose from an Algal Cell Wall. *Macromolecules*. **1991**, 24, 4168–4175.

[26] Dixon, M. C.; Quartz Crystal Microbalance with Dissipation Monitoring: Enabling Real-Time Characterization of Biological Materials and Their Interactions. *J. Biomol. Tech.* **2008,** 19(3), 151-158.

[27] Littunen, K.; Mai-Gisondi, G.; Seppälä, J.; Master, E. R. Enzymatically Debranched Xylans in Graft Copolymerization. *Biomacromolecules*. **2017**, *18*, 1634–1641.

[28] Kobayashi, T.; Taguchi, H.; Shigematsu, M.; Tanahashi, M. Substituent Effects of 3,5-Disubstituted p-Coumaryl Alcohols on Their Oxidation Using Horseradish Peroxidase-H_2O_2 as the Oxidant. *J. Wood Sci.* **2005**, *51* (6), 607–614.

[29] Uraki, Y.; Nakamura, A.; Kishimoto, T.; Ubukata, M. Interaction of Hemicelluloses with Monolignols. *J. Wood Chem. Technol.* **2007**, *27*, 9–21.

[30] Shigematsu, M.; Sugino, H.; Shinoda, Y.; Tanahashi, M. Dissolution Behavior of Monolignols in Water. *Mokuzai Gakkaishi*. **1995**, *41*(12), 1151–1157.

[31] Shigematsu, M.; Goto, A.; Yoshida, S.; Tanahashi, M.; Shinoda, Y. Hydrophobic Regions of Hemicelluloses Estimated by Fluorescent Probe Method. *Mokuzai Gakkaishi*. **1994**, *40* (11), 1214–1218.

[32] Nakamura, R.; Matsushita, Y.; Umemoto, K.; Usuki, A.; Fukushima, K. Enzymatic Polymerization of Coniferyl Alcohol in the Presence of Cyclodextrins. *Biomacromolecules*. **2006**, *7*, 1929–1934.

[33] Terashima, N.; Atalla, R. H.; Ralph, S. A.; Landucci, L. L.; Lapierre, C.; Monties, B. New Preparations of Lignin Polymer Models under Conditions That Approximate Cell Wall Lignification. *Holzforschung.* **1996**, 50, 9-14.

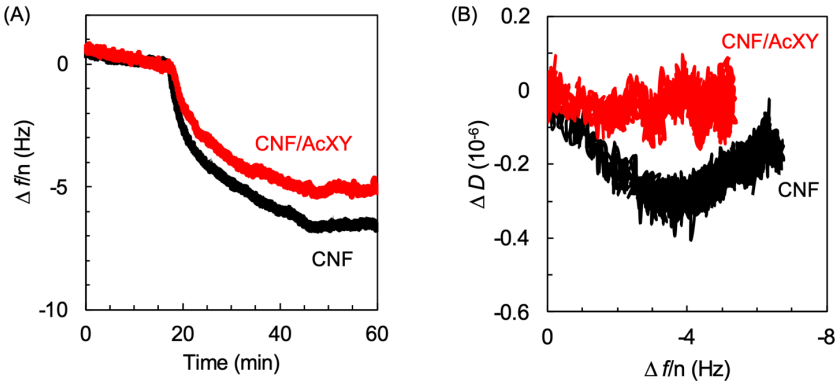

364

365 Figure 1.

366

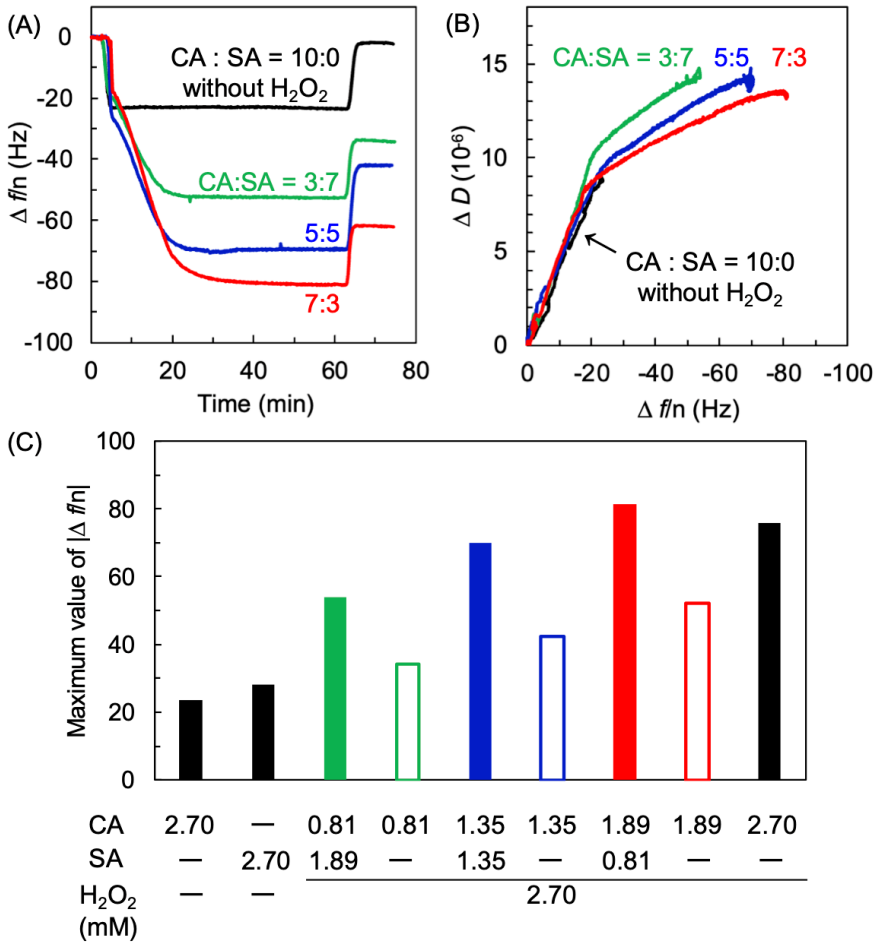

367

368 Figure 2.

369

370

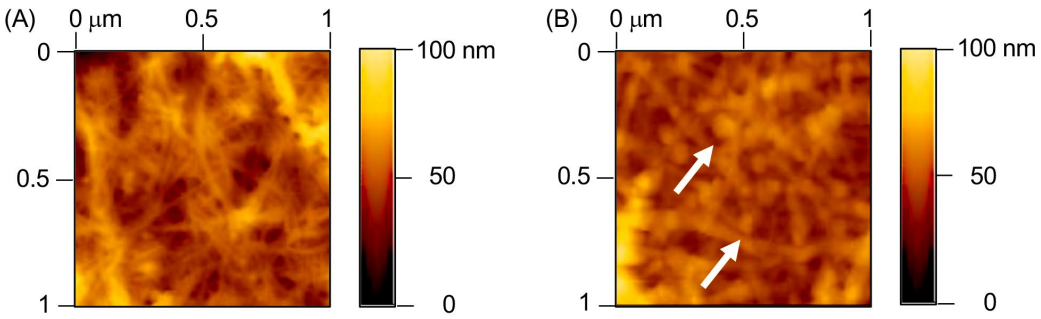

371

372 Figure 3.

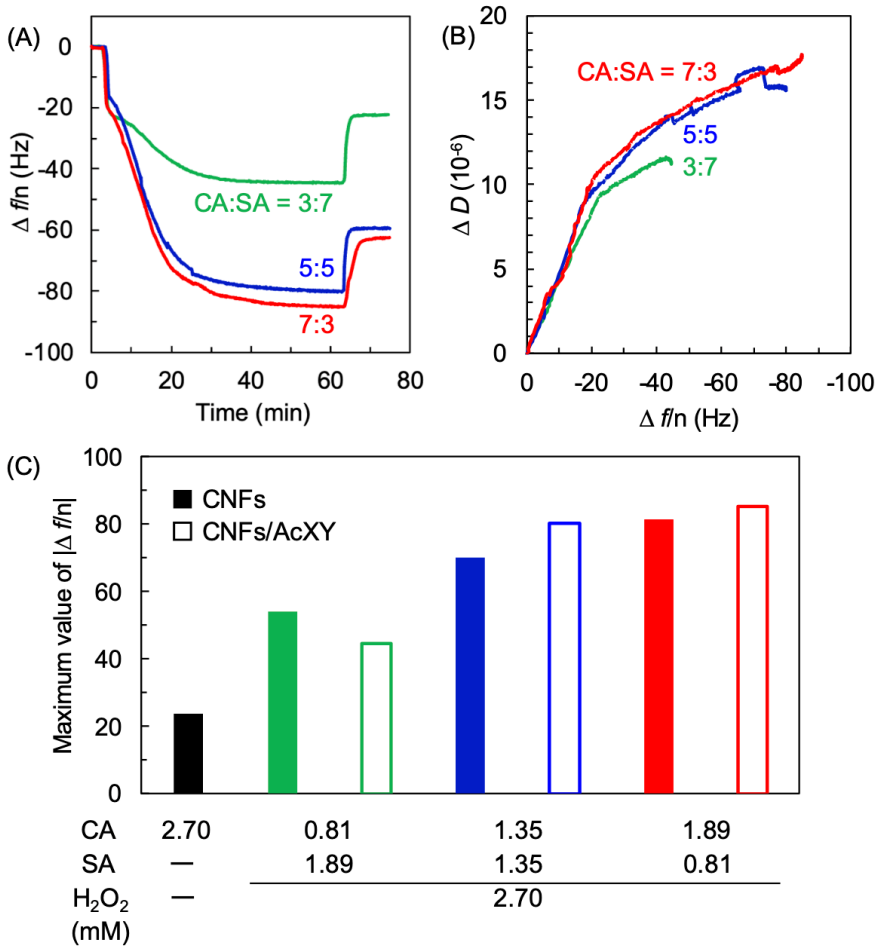

373

374 Figure 4.

375

376 Figure 1. Δ*f*/n profiles as a function of flow time and (B) Δ*D* vs. Δ*f*/n plots during HRP

377 adsorption on CNF- (black) and CNFs/AcXY-coated (red) sensor surfaces.

Figure 2. (A) Δ*f*/n profiles as a function of flow time and (B) Δ*D* vs. Δ*f*/n plots during the flow of mixtures of various molar ratios of CA and SA on CNF-coated and HRP-adsorbed sensors, performed with/without H_2O_2. (C) Maximum values of |Δ*f*/n| during the flow of mixtures of CA and SA, and only CA solutions (0.81, 1.35, 1.89 and 2.70 mM, respectively) on CNF-coated and HRP-adsorbed sensors, performed with/without H_2O_2. Molar ratios (total, 2.70 mM) of CA:SA used are 3:7 (green), 5:5 (blue), and 7:3 (red).

Figure 3. AFM images of QCM-D sensor surfaces. CNF-coated and HRP-adsorbed sensors after flowing (A) 2.70 mM of CA without H_2O_2, and (B) 1.89 mM of CA and 0.81 mM of SA with H_2O_2, where the formed DHP particles are indicated by arrows.

Figure 4. (A) Δ*f*/n profiles as a function of flow time and (B) Δ*D* vs. Δ*f*/n plots during the flow of mixtures of various molar ratios of CA and SA on CNF/AcXY-coated and HRP-adsorbed sensors, performed with/without H_2O_2. (C) Maximum values of |Δ*f*/n| during the flow of mixtures of various molar ratios (total, 2.7 mM) of CA and SA on CNF-coated (same as Figure 2C) and CNF/AcXY-coated HRP-adsorbed sensors, performed with/without H_2O_2. Molar ratios (total, 2.70 mM) of CA:SA used are 3:7 (green), 5:5 (blue), and 7:3 (red).